The *Synechocystis* Manganese Exporter Mnx Is Essential for Manganese Homeostasis in Cyanobacteria[1]

Fabian Brandenburg, Hanan Schoffman, Samantha Kurz, Ute Krämer, Nir Keren, Andreas P. M. Weber, and Marion Eisenhut

Institute of Plant Biochemistry, Cluster of Excellence on Plant Science, Heinrich Heine University, 40225 Duesseldorf, Germany (F.B., S.K., A.P.M.W., M.E.); Department of Plant and Environmental Sciences, Institute of Life Sciences, Hebrew University of Jerusalem, 91904 Jerusalem, Israel (H.S., N.K.); and Department of Plant Physiology, Ruhr University, 44801 Bochum, Germany (U.K.)

ORCID IDs: 0000-0002-5910-765X (F.B.); 0000-0002-6853-1399 (S.K.); 0000-0001-7870-4508 (U.K.); 0000-0003-0970-4672 (A.P.M.W.); 0000-0002-2743-8630 (M.E.).

The essential micronutrient manganese (Mn) functions as redox-active cofactor in active sites of enzymes and, thus, is involved in various physiological reactions. Moreover, in oxygenic photosynthetic organisms, Mn is of special importance, since it is central to the oxygen-evolving complex in photosystem II. Although Mn is an essential micronutrient, increased amounts are detrimental to the organism; thus, only a small window exists for beneficial concentrations. Accordingly, Mn homeostasis must be carefully maintained. In contrast to the well-studied uptake mechanisms in cyanobacteria, it is largely unknown how Mn is distributed to the different compartments inside the cell. We identified a protein with so far unknown function as a hypothetical Mn transporter in the cyanobacterial model strain *Synechocystis* sp. PCC 6803 and named this protein Mnx for Mn exporter. The knockout mutant Δ*mnx* showed increased sensitivity toward externally supplied Mn and Mn toxicity symptoms, which could be linked to intracellular Mn accumulation. ^{54}Mn chase experiments demonstrated that the mutant was not able to release Mn from the internal pool. Microscopic analysis of a Mnx::yellow fluorescent protein fusion showed that the protein resides in the thylakoid membrane. Heterologous expression of *mnx* suppressed the Mn-sensitive phenotype of the *Saccharomyces cerevisiae* mutant Δ*pmr1*. Our results indicate that Mnx functions as a thylakoid Mn transporter and is a key player in maintaining Mn homeostasis in *Synechocystis* sp. PCC 6803. We propose that Mn export from the cytoplasm into the thylakoid lumen is crucial to prevent toxic cytoplasmic Mn accumulation and to ensure Mn provision to photosystem II.

The transition metal manganese (Mn) plays a vital role in multiple cellular processes (Hänsch and Mendel, 2009). Mn is either part of the active site or serves as an activator for approximately 35 different enzymes (Hebbern et al., 2009). Important Mn-dependent enzymes include Mn-superoxide dismutase and Mn-catalase (Hänsch and Mendel, 2009), which serve in the detoxification of reactive oxygen species (ROS). Mn also is of central importance in carbohydrate, lipid, and lignin biosynthesis (Tobergte and Curtis, 2012). In oxygenic photosynthetic organisms, the most prominent role of Mn is in the oxygen-evolving complex (OEC) of PSII, where Mn is incorporated into a Mn_4O_5Ca cluster that mediates the splitting of water into oxygen, protons, and electrons (Nelson and Junge, 2015). While the oxygen is released, the extracted electrons are fed into the photosynthetic electron transfer chain. Thus, limited intracellular Mn content leads to a reduction of photosynthesis and growth (Salomon and Keren, 2011). However, despite its vital importance in cellular metabolism, Mn in excess amounts also can cause detrimental effects. Several Mn toxicity mechanisms are discussed, including the direct generation of ROS in a Fenton-like reaction mediated by free Mn^{2+} ions or the competition of Mn with other metal ions for incorporation into the active site of enzymes, thus changing their activity (Lynch and St. Clair, 2004). To ensure sufficient Mn supply for cellular needs while avoiding toxic overaccumulation at the same time, cellular Mn homeostasis needs to be carefully maintained, especially in oxygenic photosynthetic organisms.

In the cyanobacterium *Synechocystis* sp. PCC 6803 (hereafter *Synechocystis*), the biological role and regulation of Mn homeostasis has been partially investigated. Keren et al. (2002) demonstrated that cyanobacterial

[1] This work was supported by the German Science Foundation (grant no. EI 945/3-1 to M.E., grant no. KR 1967/3-3 to U.K., and grant no. EXC 1028 to A.P.M.W) and the Israeli Science Foundation (grant no. 2733/16 to N.K.).

*Address correspondence to m.eisenhut@uni-duesseldorf.de.

The author responsible for distribution of materials integral to the findings presented in this article in accordance with the policy described in the Instructions for Authors (www.plantphysiol.org) is: Marion Eisenhut (m.eisenhut@uni-duesseldorf.de).

F.B., M.E., N.K., and A.P.M.W. designed the study; F.B., M.E., S.K., and H.S. carried out laboratory experiments; F.B., M.E., N.K., U.K., and A.P.M.W. interpreted the data; F.B. and M.E. wrote the article; N.K., U.K., S.K., H.S., and A.P.M.W. edited and approved the article.

www.plantphysiol.org/cgi/doi/10.1104/pp.16.01895

cells contain two separate Mn pools. Up to 80% of the cellular content accumulates in the periplasmic space, probably attached to the outer membrane or bound to soluble Mn-binding proteins, such as MncA (Tottey et al., 2008). The cytoplasm was found to contain only small amounts of Mn (Keren et al., 2002). That is, the periplasm serves as an Mn storage site from where the metal is mobilized upon demand. Either Mn is imported into the cytoplasm by active transport or preloaded into PSII directly from the periplasm. The active import into the cytoplasm is mediated by the high-affinity ATP-binding cassette (ABC)-type transporter MntCAB (Bartsevich and Pakrasi, 1995, 1996), which is active only under Mn limitation conditions to provide sufficient Mn supply for cell function. The presence of a second, constitutively active but lower-affinity Mn importer in the plasma membrane also was suggested (Bartsevich and Pakrasi, 1996). Possibly, iron (Fe) transporters, such as FutABC, catalyze the transport of Mn by a piggybacking mechanism and, thus, are responsible for the constitutive Mn uptake (Sharon et al., 2014). Along with its functionality, expression of the *mntCAB* operon is under the control of a two-component regulatory system and only transcribed under Mn-limiting conditions (Ogawa et al., 2002; Yamaguchi et al., 2002). The environmental Mn availability is monitored by the Mn sensor ManS. It functions as a sensory His kinase that binds Mn^{2+} ions under Mn-sufficient conditions, autophosphorylates, and then activates the response regulator ManR by phosphorylation. In its phosphorylated state, ManR represses transcription of the *mntCAB* operon (Ogawa et al., 2002; Yamaguchi et al., 2002). Preloading of PSII with Mn^{2+} ions was demonstrated recently to be mediated by PratA, a tetratricopeptide repeat protein (Stengel et al., 2012). Since this step takes place in biogenesis centers at the cell periphery, it is assumed that Mn is loaded directly from periplasmic storage into PSII (Stengel et al., 2012) independently of internal Mn concentrations and transport activities.

In contrast to the knowledge about Mn import and its regulation, the mechanisms for managing intracellular Mn homeostasis and distribution are largely unknown in cyanobacteria. For example, intracellular Mn-binding proteins or Mn exporters have not been revealed so far. In this study, we identified and characterized a thylakoid membrane protein that is important for the export of Mn and named the protein Mnx. By the generation and characterization of a knockout mutant and overexpression line, we demonstrate that the maintenance of intracellular Mn homeostasis is highly important in *Synechocystis* and that Mnx plays a central role in Mn management. According to our results, we present a model in which Mnx is critical for mitigating cytoplasmic Mn accumulation and the provision of Mn to the OEC, thus maintaining efficient photosynthesis.

RESULTS

Identification of a Candidate Mn Transporter

Since Mn is of central importance especially in all organisms performing oxygenic photosynthesis, we assumed that the transport protein should be conserved throughout cyanobacteria, algae, and land plants. Thus, to search for a candidate Mn exporter, we explored the inventory of the so-called GreenCut2, which comprises a set of all proteins that are encoded in the genomes of Viridiplantae (green algae and land plants) but not in or highly diverged in the genomes of nonphotosynthetic organisms (Karpowicz et al., 2011). Among the 597 GreenCut proteins in the green alga *Chlamydomonas reinhardtii*, which is used as a reference organism for the GreenCut, 83 proteins are assigned to the functional category transport, 45 with known and 38 with unknown functions (Karpowicz et al., 2011). We concentrated only on those proteins that were predicted to localize to the chloroplast in Viridiplantae, were of unknown function, and were strictly conserved, meaning encoded in at least 95% (at least 35 of 37 analyzed genomes; Karpowicz et al., 2011) of the analyzed cyanobacterial genomes. The final set of five transport proteins (Supplemental Table S1) contained the protein CPLD63, which belongs to the unknown protein family 0016 (UPF0016). This GreenCut protein seemed to be a promising candidate, since another member of UPF0016, the Gcr1-dependent translation factor1 (GDT1), was proposed to function as a Golgi-localized Ca^{2+}/H^{+} antiporter in yeast (*Saccharomyces cerevisiae*; Demaegd et al., 2013), and Ca^{2+}-transporting systems are known to frequently also accept Mn^{2+} as a substrate (Socha and Guerinot, 2014). The *Synechocystis* genome contains the gene *sll0615*, encoding an orthologous protein to CPLD63. Thus, we selected Sll0615 as a candidate protein to test for Mn export function in the cyanobacterium and designated Sll0615 as Mnx.

Deletion of Mnx Results in Sensitivity toward Externally Supplied Mn

To test the function of Mnx, we generated a *Synechocystis* mutant line, Δ*mnx*, by insertional inactivation (Fig. 1A). Full segregation of the Δ*mnx* mutant line and the complete loss of *mnx* transcripts (Fig. 1, B and C) demonstrated that Mnx was not essential under the standard conditions used. Additionally, we generated a complementation line, Δ*mnx/OEX*, in which the expression of *mnx* is under the control of the strong *psbAII* promoter (Lagarde et al., 2000) in the Δ*mnx* mutant background (Fig. 1, A and B). According to real-time quantitative PCR (RT-qPCR) analysis, the abundance of *mnx* transcript was 7-fold elevated in the Δ*mnx/OEX* line compared with the wild type (Fig. 1C). Therefore, this line was considered as both a complementation line and an overexpression line.

We hypothesized that Mnx functions as an Mn exporter. Thus, we tested the mutant for sensitivity toward externally supplied Mn. When we treated the cells with increasing Mn concentrations, we observed that the Δ*mnx* mutant was not able to grow on BG11 medium with elevated Mn concentration (Fig. 2A). The commonly used BG11 medium (Rippka et al., 1979) contains 9 μM $MnCl_2$. At this concentration and on medium without $MnCl_2$ (0 μM), wild-type and Δ*mnx* cells grew comparably

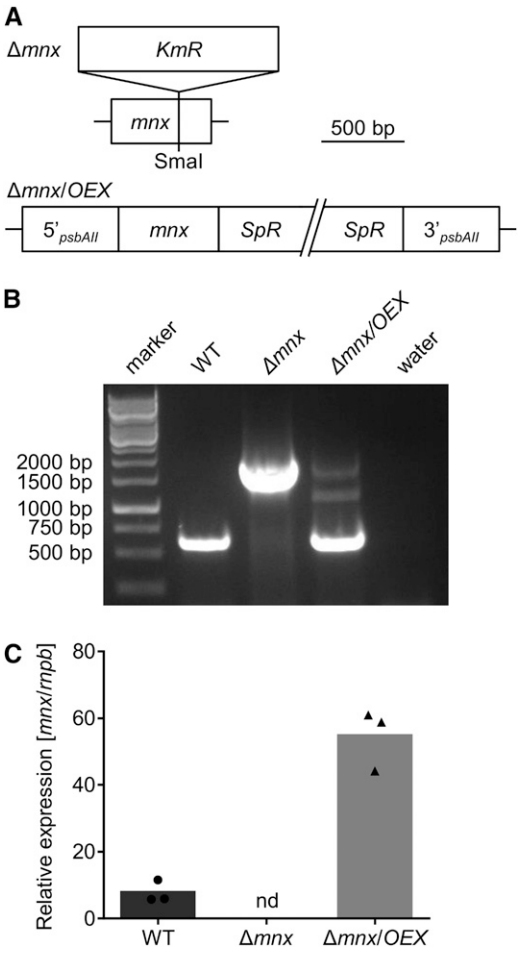

Figure 1. Generation of *mnx* knockout and overexpression lines. A, The knockout mutant Δ*mnx* was generated by insertion of a kanamycin resistance cassette (*KmR*) into the coding sequence of the *mnx* gene at the unique *Sma*I restriction site. The overexpression line Δ*mnx/OEX* was generated by reintroducing *mnx* under the control of the strong *psbAII* promoter into the genetic background of Δ*mnx*. Using homologous recombination, *mnx* was integrated into the *psbAII* locus. For selection, a gene encoding a spectinomycin resistance cassette (*SpR*) was included. B, The genotypes of the mutants were verified by PCR using gene-specific primers for amplification of *mnx*. Water was used as a negative control. WT, Wild type. C, The transcript abundance of *mnx* was analyzed by RT-qPCR. nd, Not detectable.

well. However, in response to a slightly increased concentration of 12.5 μM $MnCl_2$, growth of the mutant was retarded, while higher concentrations of $MnCl_2$ resulted in a lethal phenotype of the Δ*mnx* mutant. The rescued growth of the Δ*mnx/OEX* line proved that the Mn sensitivity was indeed caused by the loss of Mnx and not by any secondary mutation (Fig. 2A). We also tested the sensitivity toward additional divalent transition metals, since Mn transporters are known at least in plants as being promiscuous for their substrates (Socha and Guerinot, 2014). Growth of the Δ*mnx* mutant was not distinguishable from that of the wild type in response to 12.5-fold elevated concentrations of Ca^{2+} ions or 3-fold Fe^{2+}, Cu^{2+}, Zn^{2+}, and Co^{2+} ions in the BG11 medium (Fig. 2B). Also, the addition of Cd^{2+} or Ni^{2+} ions, which are not contained in standard BG11 medium, did not affect the growth of the Δ*mnx* mutant. The dose-dependent and metal-specific phenotype observed here provided, to our knowledge, the first indications that Mnx conveys resistance to elevated Mn amounts, likely by a specific export of Mn.

The Δ*mnx* Mutant Shows Symptoms of Mn Toxicity

The Mn-dependent phenotype of the mutant was studied in more detail. To implement Mn limitation conditions, we precultivated all lines in BG11 medium without Mn. Mn depletion for 5 d did not restrict growth or chlorophyll content in any strain (Fig. 3, A–C). After preincubation, the cultures were supplemented with either 9 or 150 μM $MnCl_2$ to apply standard or high Mn concentrations (Fig. 3, B and C). As a control, the Mn limitation conditions were continued (Fig. 3A). Application of both 0 and 9 μM $MnCl_2$ did not affect the growth and chlorophyll amounts in either culture (Fig. 3, A and B; Supplemental Fig. S1, A and B). However, after the addition of 150 μM $MnCl_2$, growth of the Δ*mnx* mutant was impaired and also chlorophyll amounts decreased significantly (Fig. 3C; Supplemental Fig. S1, A and B). The negative effect of the high-Mn treatment on Δ*mnx* cells was additionally reflected by strongly reduced photosynthetic activity, as indicated by reduced oxygen evolution (Fig. 3D). Under Mn-depleted conditions, oxygen evolution was not significantly different between the lines. However, 4 h after the addition of 9 μM $MnCl_2$, oxygen evolution was reduced significantly by 30%, and 4 h after the addition of 150 μM $MnCl_2$, it was reduced significantly by 70% (Fig. 3D). In contrast, the overexpression line Δ*mnx/OEX* showed a significant increase in photosynthesis 4 h after the addition of 9 μM $MnCl_2$ or 150 μM $MnCl_2$ compared with the wild type (Fig. 3C). Importantly, the significant difference between the wild type and the overexpression line results from a decrease in the activity of the wild type with increasing concentration of Mn but not from an increase in photosynthesis of the overexpression line (Fig. 3D). The detrimental effect of 150 μM $MnCl_2$ on the growth of Δ*mnx* cells is shown in Figure 3E.

The Δ*mnx* Mutant Mounts a High-Light-Sensitive Phenotype

The observation that photosynthetic activity was affected after the addition of $MnCl_2$ in the Δ*mnx* mutant prompted us to investigate the inhibition mechanism in more detail. We did not observe significantly reduced photosynthetic activity under Mn depletion (Fig. 3D) and, thus, expected that the negative effect of Mn in the Δ*mnx* mutant was not due to reduced incorporation of Mn into de novo assembled PSII but rather was caused by Mn-dependent effects on the photosynthesis apparatus. To test this hypothesis, we analyzed the lines at standard Mn concentrations (9 μM) but two different light intensities. Our standard growth light conditions were 100 μmol photons m^{-2} s^{-1}. For high-light conditions,

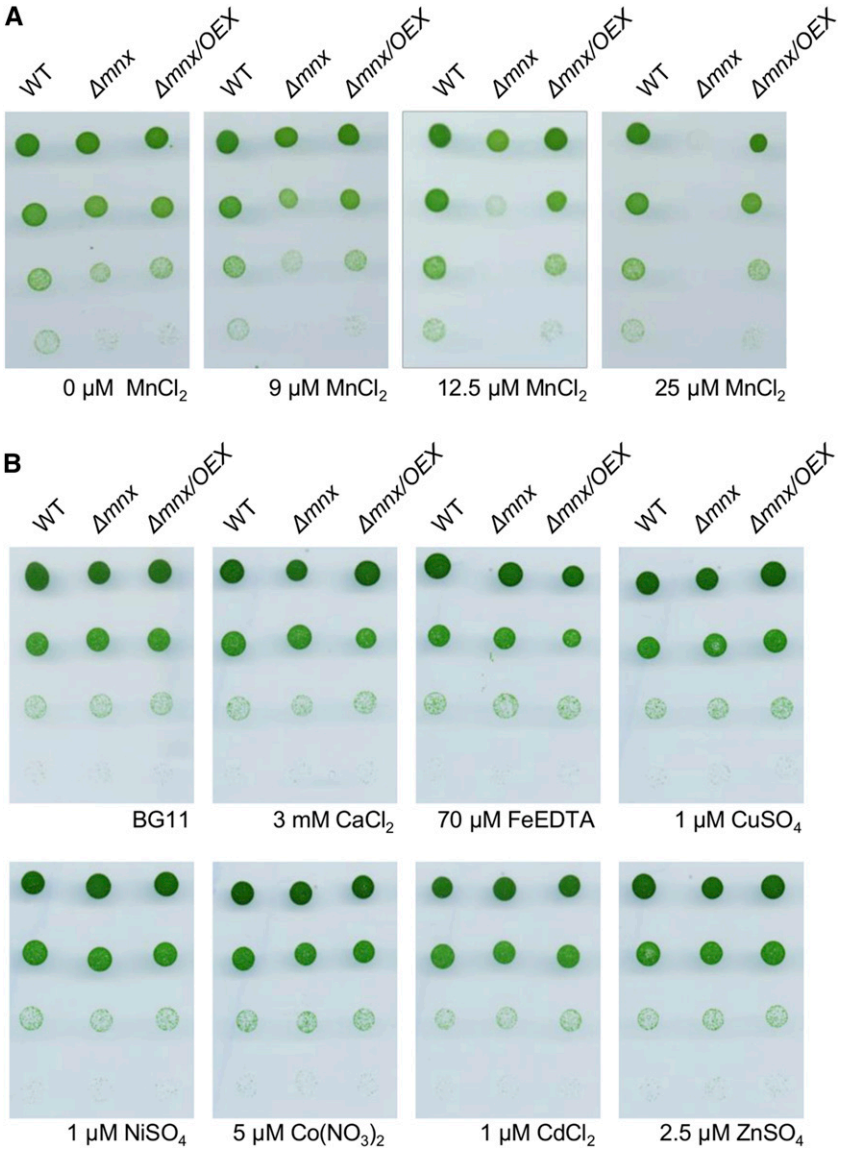

Figure 2. Sensitivity of *Synechocystis* wild type (WT), Δ*mnx* mutant, and Δ*mnx/OEX* line toward divalent transition metals. Cells of the mid log phase were diluted to an optical density at 750 nm (OD_{750}) of 0.25. Two microliters of these cultures and subsequent 1:10, 1:100, and 1:1,000 dilutions were spotted onto BG11 plates supplemented with different transition metals as indicated. Photographs were taken after incubation for 4 d. A, Growth of cells on BG11 medium containing 0, 9, 12.5, or 25 μM $MnCl_2$. Nine micromolar is the standard concentration of $MnCl_2$ in BG11 medium. B, Growth of cells on BG11 medium containing elevated levels of divalent transition metals. The concentrations were 12.5-fold elevated for Ca^{2+} and 3-fold elevated for Fe^{2+}, Cu^{2+}, Zn^{2+}, and Co^{2+} ions compared with standard BG11 medium. Additionally, Cd^{2+} and Ni^{2+} ions were tested, which are not contained in standard BG11 medium.

the cultures were exposed to a light intensity of 1,000 μmol photons m^{-2} s^{-1}. Similar to the results of the Mn treatment (Fig. 3), Δ*mnx* was impaired significantly in growth and chlorophyll content under high-light conditions (Fig. 4, A and B; Supplemental Fig. S1, C and D). Also, the photosynthetic activity in the Δ*mnx* mutant was reduced significantly after 4 h of high-light treatment (Fig. 4C). To distinguish whether photoinhibition or recovery was changed due to the lack of Mnx, all three lines were first incubated in BG11 medium containing the standard 9 μM $MnCl_2$ under high-light conditions for 45 min and then shifted back to standard growth light conditions. Oxygen evolution was measured to determine photosynthetic activity. While the photoinactivation rate was comparable between the wild type, the Δ*mnx* mutant, and the Δ*mnx/OEX* line (Fig. 4D), the recovery time was increased significantly for Δ*mnx*. The mutant needed 2.7 times longer to recover to 50% of its initial photosynthetic rate (Fig. 4E). The detrimental effect of 1,000 μmol photons m^{-2} s^{-1} on the growth of Δ*mnx* cells is shown in Figure 4F.

Lack of Mnx Leads to an Increased Intracellular Mn Pool

Both reduced chlorophyll accumulation (Csatorday et al., 1984; Clairmont et al., 1986) and photosynthetic activity (Millaleo et al., 2013) were described earlier as typical symptoms of critical Mn accumulation in oxygenic photosynthetic organisms. To investigate whether the observed phenotype of the Δ*mnx* mutant was caused by Mn accumulation, we quantified the cellular Mn amounts. The intracellular Mn pools were reduced strongly after 5 d of Mn depletion treatment and not significantly different between the three lines (Fig. 5). Significant overaccumulation (3-fold) in the intracellular Mn pool was observed specifically for the Δ*mnx* mutant after Mn addition, while the intracellular Mn levels of the Δ*mnx/OEX*

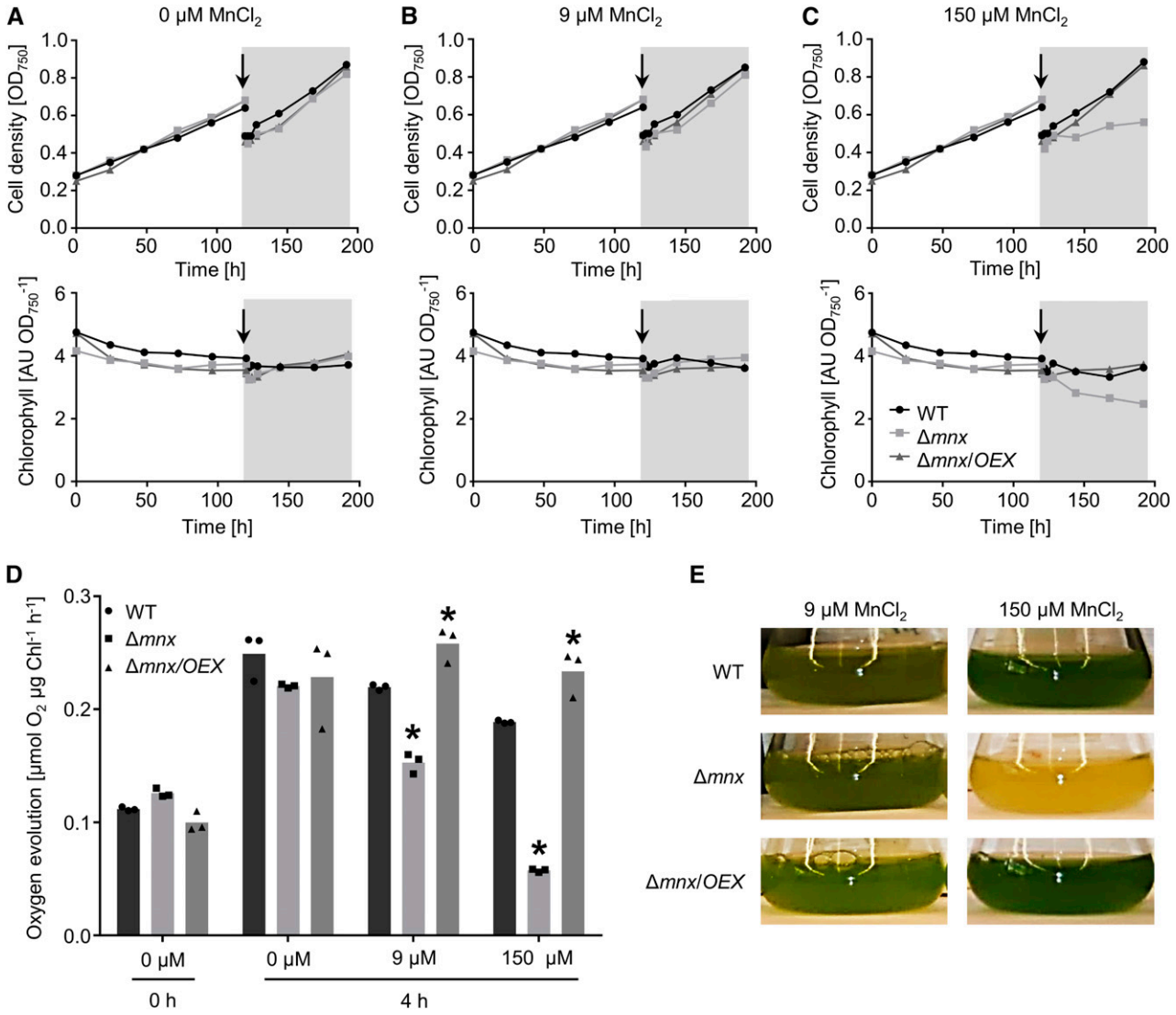

Figure 3. Effects of Mn treatment on physiological parameters of the wild type (WT), Δ*mnx* mutant, and Δ*mnx/OEX* line. A to C, During the first 5 d, the cultures were grown in Mn-free medium (white areas). For the remaining 3 d, the cultures were diluted and treated with 0 μM (A), 9 μM (B), or 150 μM (C) $MnCl_2$. Growth (top row) and chlorophyll content (bottom row) were monitored over a time course of 8 d. The addition of $MnCl_2$ is indicated with the arrows and the gray areas. One representative result of four independent experiments is shown. D, Before (0 h) and 4 h after treatment, additional samples were taken for oxygen evolution measurements. Values shown are means of three independent experiments. Asterisks indicate significant changes to the respective wild-type value according to a two-way ANOVA ($P \leq 0.05$). E, Mn-dependent lethal phenotype of the Δ*mnx* mutant. Shown are photographs of the cultures after 3 d of growth in BG11 medium containing 9 or 150 μM $MnCl_2$. AU, Arbitrary units.

line and the wild type were equal (Fig. 5). Thus, the intracellular Mn levels provided further evidence that Mnx is involved in Mn export out of the cell.

Loss of Intracellular ^{54}Mn Is Impaired in the Δ*mnx* Mutant

To examine whether, in fact, the export was affected by the loss of *mnx*, we performed in vivo ^{54}Mn chase experiments (Fig. 6). After the cells had been incubated for 3 d in BG11 medium supplemented with ^{54}Mn, which allowed the incorporation of ^{54}Mn into internal pools and into proteins, cells were washed and further cultivated in BG11 medium without the radioactive isotope. During the whole experiment, the final concentration of $MnCl_2$ was kept constantly at the standard 9 μM. In all three lines, the intracellular signal of the radioactive ^{54}Mn isotope declined most strongly within the first 30 min. However, the ^{54}Mn contents in the Δ*mnx* mutant stably remained at 80% of the starting amount. In contrast, wild-type and Δ*mnx/OEX* cells displayed a monotonous decrease of the radioactive signal. The decrease of ^{54}Mn in wild-type and Δ*mnx/OEX* cells was significantly higher throughout the whole experiment in comparison with the Δ*mnx* mutant, with a total loss of ~80% of the

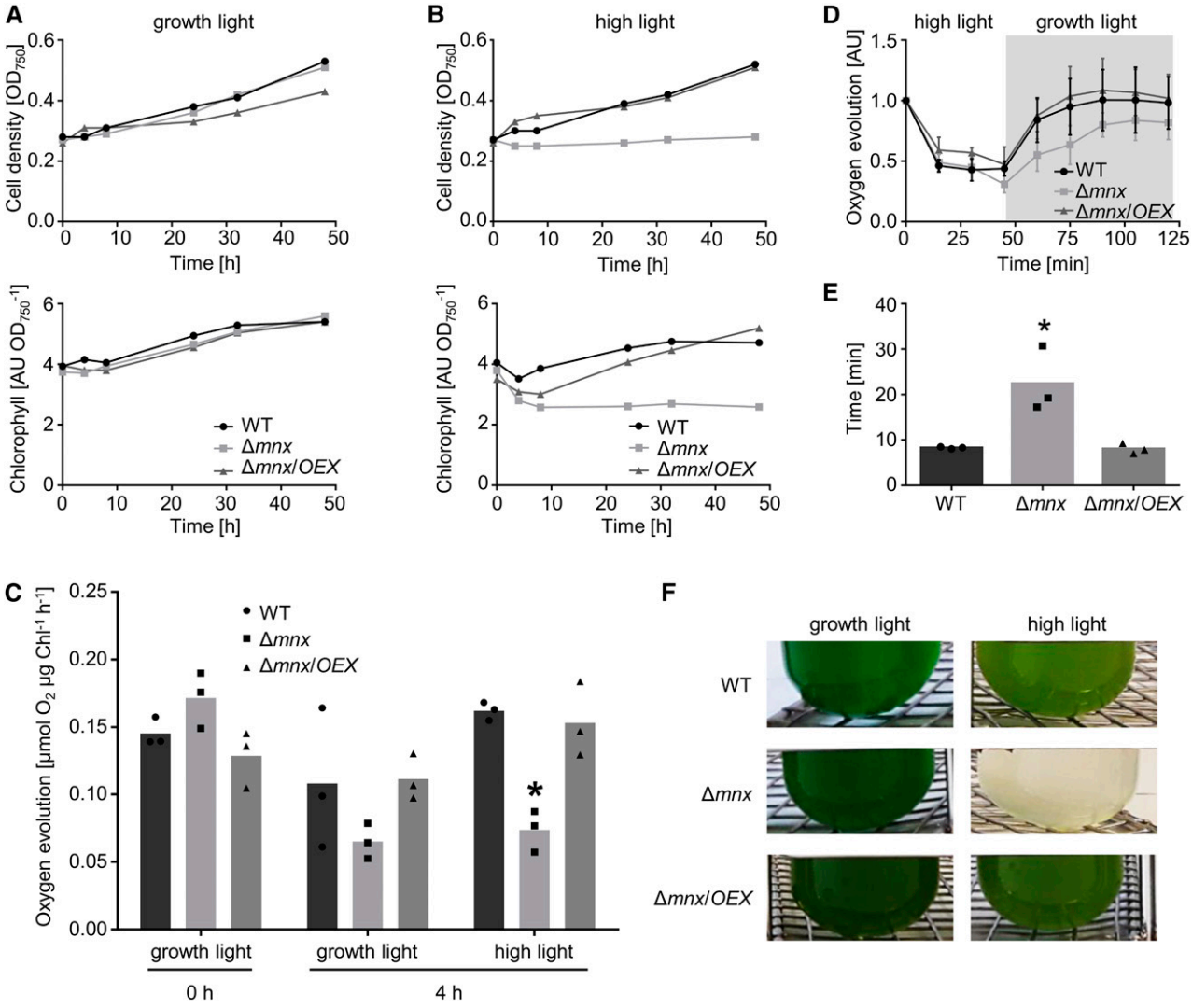

Figure 4. Effects of high-light treatment on physiological parameters of the wild type (WT), Δ*mnx* mutant, and Δ*mnx/OEX* line. A and B, The cultures were grown either under standard growth light (100 μmol photons m^{-2} s^{-1}; A) or high-light (1,000 μmol photons m^{-2} s^{-1}; B) conditions. Growth (top row) and chlorophyll content (bottom row) were monitored over a time course of 48 h. C, Additional samples were taken before (0 h) and 4 h after exposure to growth light and high-light conditions, respectively, for oxygen evolution measurements. Values shown are means of three independent experiments. D, For photoinhibition and recovery studies, cultures were shifted to high-light (1,000 μmol photons m^{-2} s^{-1}; white area) conditions. After 45 min, the cultures were shifted back to 100 μmol photons m^{-2} s^{-1} (gray area) and the recovery of photosynthetic activity was monitored. Means and SD of three independent experiments are shown as the oxygen evolution relative to the corresponding time point 0 min for each line. E, The time that each culture needs for one-half-maximal recovery was calculated from D. F, The high-light-dependent lethal phenotype of the Δ*mnx* mutant. Shown are photographs of the cultures after 48 h of growth under growth light (100 μmol photons m^{-2} s^{-1}) or high-light (1,000 μmol photons m^{-2} s^{-1}) conditions. Asterisks indicate significant changes to wild-type values according to a two-way ANOVA ($P \leq 0.05$). AU, Arbitrary units.

radioactive signal for both the wild type and the overexpression line Δ*mnx/OEX* within the 4-h course (Fig. 6).

Mnx Resides in the Thylakoid Membrane

To investigate the subcellular localization of the Mnx protein, we generated a mutant line, *mnx*::*yfp*, expressing a Mnx protein with a C-terminal enhanced yellow fluorescent protein (eYFP) fusion. The biological functionality of the Mnx::YFP fusion proteins was confirmed by demonstrating unrestricted growth of the *mnx*::*yfp* line at Mn concentrations that are lethal for the Δ*mnx* mutant (Supplemental Fig. S2B). For confocal fluorescence microscopy, we mixed *mnx*::*yfp* and wild-type cells to have both cell lines on the same image. The YFP signal showed a complete overlap with the chlorophyll autofluorescence signal, indicating the localization of Mnx::YFP in the thylakoid membrane. In some cases,

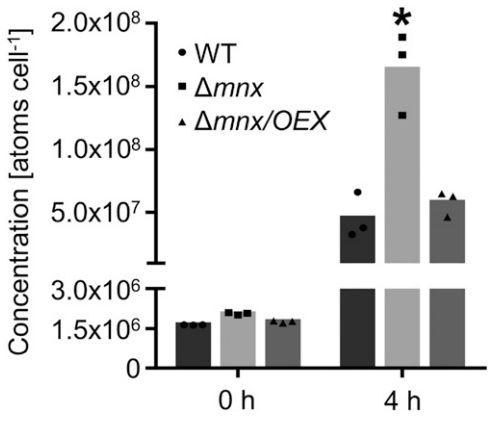

Figure 5. Intracellular Mn accumulation in the wild type (WT), Δ*mnx* mutant, and Δ*mnx/OEX* line. Cells were grown under Mn-limiting conditions for 5 d and then treated with 200 μM $MnCl_2$. Inductively coupled plasma mass spectrometry (ICP-MS) analysis was performed after starvation (0 h) and 4 h after treatment with $MnCl_2$. Each bar represents three biological replicates. The asterisk indicates a significant change to the respective wild-type value according to a two-way ANOVA ($P \leq 0.05$).

we observed locally increased YFP signals (Fig. 7). To analyze the spatial distribution in more detail, we furthermore quantified the signal intensities of a circumferential profile for the two *mnx*::*yfp* cells and found the YFP and chlorophyll autofluorescence signals positively correlated (Supplemental Fig. S3B). A slight patchiness with regard to the YFP signal also was observed for both cells. We detected regions where the autofluorescence was low while YFP fluorescence peaked (Supplemental Fig. S3B). For wild-type cells, we did not detect a signal in the YFP channel with the settings used (Fig. 7). The different intensities in the autofluorescence probably resulted from the unequal arrangement of *mnx*::*yfp* and wild-type cells, with the wild-type cells being ~0.2 μm increased in comparison with the wild type cells (Supplemental Fig. S3).

Expression of Mnx Suppresses the Phenotype of a Yeast Mn Transport Mutant

To further prove that Mnx facilitates the transport of Mn and does not act as a regulatory Mn receptor protein, we employed a heterologous yeast mutant suppression assay. In *Saccharomyces cerevisiae* cells, Mn^{2+} and Ca^{2+} ions are imported into the secretory pathway by a P-type Ca^{2+}/Mn^{2+} ATPase, PMR1, that resides in the Golgi apparatus membrane (Dürr et al., 1998). The corresponding mutant Δ*pmr1* accumulates Mn in the cytoplasm (Lapinskas et al., 1995) and cannot survive on medium containing 2 mM $MnCl_2$ (Maeda et al., 2004). Heterologous expression of the cyanobacterial Mnx protein suppressed the Mn-sensitive phenotype of the Δ*pmr1* mutant (Fig. 8), which strongly supports a role of Mnx in Mn export from the cytoplasm.

DISCUSSION

Mnx Facilitates the Export of Mn from the Cytoplasm in *Synechocystis*

Mn homoeostasis in oxygenic photosynthetic organisms needs to be carefully sustained to avoid limited provision of Mn^{2+} ions to the OEC of PSII, on the one hand, and inhibitory effects due to cytoplasmic Mn accumulation, on the other hand. In search of an Mn exporter in the cyanobacterium *Synechocystis*, we identified the protein Mnx encoded by the open reading frame *sll0615* as a promising candidate. In this study, we provide several independent lines of evidence that Mnx, in fact, functions in the export of Mn from the cytoplasm.

The knockout mutant Δ*mnx* showed high sensitivity toward externally supplied Mn. Already, a treatment with only 1.4-fold elevated $MnCl_2$ concentration (12.5 μM) had a strong negative impact on the mutant, while a 2.8-fold concentration (25 μM) was lethal for Δ*mnx* (Fig. 2A). Different physiological mechanisms for Mn toxicity were suggested. First, Mn can compete with other divalent metal ions, such as magnesium, Fe, or calcium (Ca), for incorporation into the active sites of enzymes and, thus, modifies enzymatic activities. For this reason, chlorophyll biosynthesis is inhibited in cyanobacteria (Csatorday et al., 1984) and plants (Clairmont et al., 1986) upon Mn intoxication. Furthermore, excess Mn inhibits Rubisco activity (Houtz et al., 1988; Nable et al., 1988) and photosynthetic activity (Millaleo et al., 2013) for the same reason. Second, free Mn possibly functions as a redox-active metal in a Fenton-like reaction with the generation of most reactive OH· radicals. However, it is assumed that, in vivo, the reduction potential of Mn is not low enough to catalyze this toxic reaction (Kehres and Maguire, 2003). Our physiological analyses revealed that the mutant line Δ*mnx* showed several of the described symptoms of Mn toxicity. Chlorophyll accumulation in Δ*mnx* cells was reduced after the application of Mn (Fig. 3, B and C; Supplemental Fig. S1B), likely as a consequence of Mn-inhibited chlorophyll biosynthesis. Also, photosynthetic activity was lower in the mutant as a function of external Mn concentration (Fig. 3D). The enhanced generation of OH· radicals was not investigated in this study and cannot be excluded as another reason for the lethality of Δ*mnx* cells upon exposure to high Mn concentrations.

ICP-MS analysis (Fig. 5) supported the hypothesis that the observed physiological symptoms were actually caused by intracellular Mn overaccumulation in the Δ*mnx* mutant. The intracellular Mn level was 3-fold higher in Δ*mnx* than in wild-type cells, and this elevation was obviously sufficient to negatively influence the performance of the mutant cells. Similar behavior was observed for a mutant in the plasma membrane Mn efflux system, MntE, in *Streptococcus pneumoniae*. Incubation with 300 μM $MnCl_2$ resulted in 5-fold increased intracellular Mn amounts compared with wild-type cells, and high Mn concentrations in the growth medium led to severe growth inhibition (Rosch et al., 2009). Our results are in the same range and demonstrate the strict need for the maintenance of Mn homeostasis.

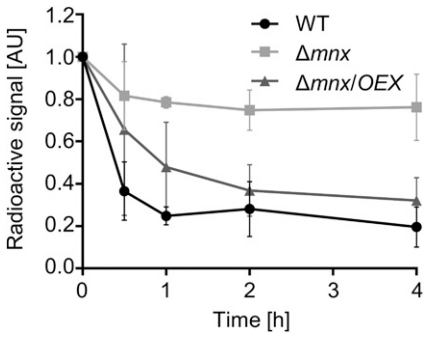

Figure 6. Radioactive trace experiments. Cells limited for Mn were incubated with radioactive ^{54}Mn for 3 d. After washing and transfer to label-free BG11 medium, the decay of the radioactivity signal was followed over a time course of 4 h. Radioactivity at time point 0 h was set to 100%, and subsequent values were normalized to this time point. Values shown are means and SD of three biological replicates. WT, Wild type; AU, arbitrary units.

Also, mutants in the Mn uptake regulatory system, ManSR, showed intracellular Mn accumulation and symptoms of intoxication upon high-Mn treatment (Zorina et al., 2016), which, in the *manS* and *manR* mutants, is essentially caused by uncontrolled Mn uptake via the Mn ABC-type transporter MntCAB (Bartsevich and Pakrasi, 1995). According to DNA microarray analysis of these mutants, *mnx* expression is not controlled by the two-component system ManSR (Yamaguchi et al., 2002). To prove that the membrane protein Mnx is not a Mn sensor but functions as a translocator, we employed a yeast mutant phenotype suppression assay. The strong growth phenotype of the Mn-sensitive yeast mutant Δ*pmr1* (Maeda et al., 2004) could be suppressed on Mn-containing medium by the expression of *Synechocystis mnx* (Fig. 8). Thus, we suggest that Mnx, indeed, functions as a transporter and not as a signaling or regulatory protein.

The measured intracellular Mn content comprises the Mn pools of cytoplasm, thylakoid membrane, and thylakoid lumen. Accordingly, three alternative hypotheses for Mnx function are conceivable: Mnx facilitates Mn export from the cytoplasm into (1) the periplasm, (2) the thylakoid lumen, or (3) export from the thylakoid lumen into the cytoplasm. To distinguish between these options, we determined the subcellular localization of Mnx. According to the fluorescence microscopy images (Fig. 7), Mnx resides in the thylakoid membrane, which is in agreement with a recent global proteomics study in *Synechocystis* (Liberton et al., 2016), finding Mnx essentially in the thylakoid membrane fraction. However, we cannot rule out that minor amounts of Mnx also reside in the plasma membrane. In Arabidopsis (*Arabidopsis thaliana*), the homologous protein PHOTOSYNTHESIS AFFECTED MUTANT71 (PAM71) resides in the thylakoid membrane as well (Schneider et al., 2016). PAM71 is suggested to facilitate Mn uptake from the chloroplast stroma into the thylakoid lumen in antiport with protons, thus providing Mn for incorporation into the OEC of PSII (Schneider et al., 2016). For other members of the UPF0016, a proton-coupled antiport mode is proposed (Demaegd et al., 2013). In accordance, we anticipate that Mnx serves in Mn transport from the cytoplasm to the thylakoid lumen of illuminated *Synechocystis* cells.

We observed phenotypic changes only upon treatment with Mn. All other divalent metals tested, Ca^{2+}, Fe^{2+}, Cu^{2+}, Ni^{2+}, Co^{2+}, Cd^{2+}, or Zn^{2+}, did not negatively impact the Δ*mnx* mutant (Fig. 2B), indicating that Mnx facilitates the transport of Mn with rather high specificity. This high specificity of Mnx for Mn was surprising, since metal transporters are typically promiscuous regarding their substrate (Socha and Guerinot, 2014). For example, members of the NRAMP family transport a broad range of metals. For the Arabidopsis proteins AtNRAMP3 and AtNRAMP4, a function in both Fe and Mn transport was demonstrated (Lanquar et al., 2005, 2010). However, since it is conceivable that, for some metals, such as Ca or Fe, more efficient compensatory mechanisms exist than for Mn, and for that reason we do not see any effect, we cannot rule out that other metals also are transported by Mnx.

Toward the Biological Function of Mnx in Cyanobacteria

The current knowledge about proteins involved in cellular Mn homeostasis is described in the introduction and summarized in Figure 9. We have identified Mnx as a new player in the management of cyanobacterial Mn homoeostasis that facilitates Mn transport from the cytoplasm into the thylakoid lumen. However, what is the critical biological function of Mn export from the cytoplasm into the thylakoid lumen?

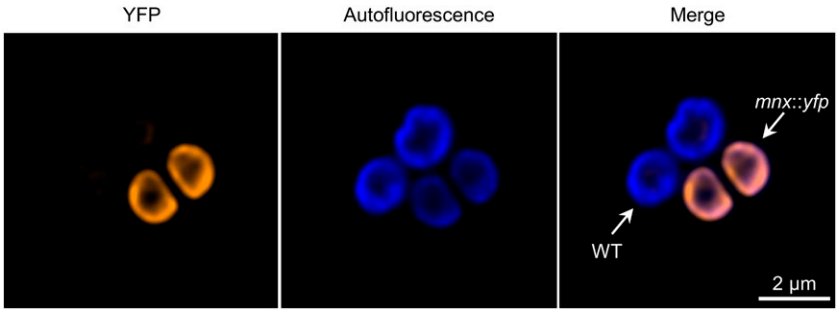

Figure 7. Subcellular localization of the Mnx::YFP protein. *mnx*::*yfp* cells, expressing the Mnx protein with a C-terminal fusion to YFP, were mixed with wild-type (WT) cells as a negative control and inspected by confocal fluorescence microscopy. YFP fluorescence is shown in orange and chlorophyll autofluorescence in blue. Shown is stack 5 of a total series of nine z-stacks. The complete series of z-stacks is shown in Supplemental Figure S3.

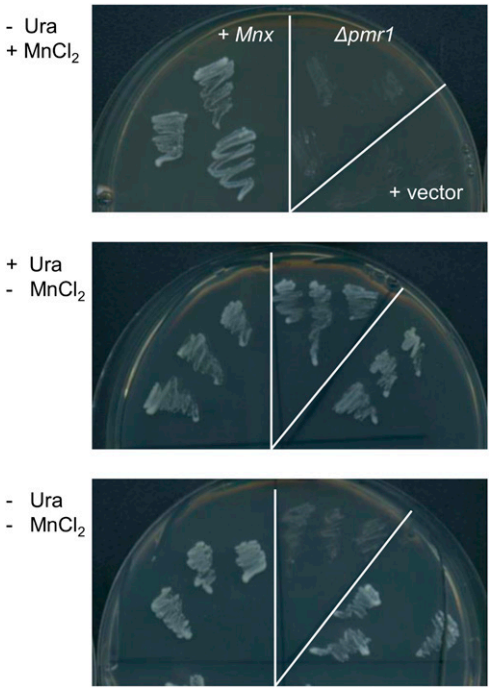

Figure 8. Expression of *Synechocystis mnx* in the *S. cerevisiae* mutant Δ*pmr1*. Mutant Δ*pmr1* cells, Δ*pmr1* cells containing the empty vector pDR196 (+ vector), and Δ*pmr1* cells carrying the vector with *mnx* as an insert (+ *Mnx*) were verified by PCR and streaked on synthetic medium with (+) or without (−) 2 mM $MnCl_2$. For selection, uracil (Ura) was added (+) or omitted (−). Photographs were taken after 4 d of incubation at 30°C.

Function 1

Mnx sequesters free Mn into the thylakoid lumen to mitigate harmful effects. Cytoplasmic Mn accumulation leads to detrimental effects, as discussed above, and needs to be avoided. Thus, Mn is sequestered by the Mnx protein into the thylakoid lumen, where Mn likely does no harm. High environmental Mn concentrations, as provided in our experimental setup, lead to cytoplasmic Mn accumulation. Since Mn concentrations in aquatic habitats are in the range of 0.1 to 10 nM (Salomon and Keren, 2015), this scenario is not very likely to occur in nature. Alternatively, cytoplasmic Mn accumulation could result from the release of this metal during protein turnover and degradation. According to our results, the major path to eliminate intracellular Mn basically involves Mnx and passage through the thylakoid lumen. In our ^{54}Mn chase experiments, the knockout mutant Δ*mnx* retained about 80% of the intracellular radioactive signal, while in the wild type and the overexpression line, the signal decreased rapidly to about 20% (Fig. 6). Thus, the data show that more than 70% of the internal Mn pool is rapidly turned over and exported to the periplasm within 1 h in wild-type and Mnx overexpression cultures (Fig. 6). The remaining approximately 20% of the intracellular Mn pool is probably bound to proteins that are stable over the observed period of time. Furthermore, the results indicate that Δ*mnx* is unable to export Mn resulting from intracellular protein turnover even under unstressed conditions (i.e. 9 μM $MnCl_2$ in the standard BG11 medium). Every cell division causes a dilution of cytoplasmic Mn, which likely contributes to mutant survival in the standard conditions. The intriguing result that Mnx contributes significantly to the release of Mn into the periplasm, although the transporter resides in the thylakoid membrane, remains to be explained. Interestingly, a similar behavior was demonstrated for a mutant in the thylakoid Na^+/H^+ transporter Nhas3 in *Synechocystis*. Although the transporter resides in the thylakoid membrane, the *nhaS3* knockdown mutant showed increased sensitivity toward elevated Na^+ concentrations in the medium (Tsunekawa et al., 2009).

Function 2

Mnx contributes to Mn supply to the OEC. In cyanobacteria, major intracellular Mn amounts presumably are contained in the Mn_4O_5Ca cluster of the OEC, since, in chloroplasts, roughly 80% of Mn is associated with PSII (Anderson et al., 1964). The cluster is bound by the D1 protein and stabilized by the extrinsic, lumenal PSII subunits PsbO, PsbP, PsbQ, PsbU, and PsbV in cyanobacteria (Nickelsen and Rengstl, 2013). It is suggested that the loading of pre-D1 protein with Mn takes place in biogenesis centers and is mediated by the PratA protein (Stengel et al., 2012). The D1 protein is damaged continuously by light and needs to be repaired (i.e. replaced by de novo synthesized D1). To allow for PSII repair, PSII is disassembled and the photodamaged D1 is removed by proteases (for review, see Nickelsen and Rengstl, 2013). Concomitantly, the Mn_4O_5Ca cluster is released into the thylakoid lumen. It is debated whether the de novo synthesized D1 can be inserted into PSII in thylakoid membranes or whether the repair takes place at the biogenesis centers with the participation of PratA (Nickelsen and Rengstl, 2013). It is also not clear whether the released Mn can be recycled or needs to be replaced by freshly imported Mn. Our observations that the Δ*mnx* mutant was highly susceptible to high light intensities (Fig. 4) and needed significantly longer to recover from a short-time high-light treatment (Fig. 4, D and E) are indications that, at least partly, the repair of PSII occurs on site and employs Mnx to import Mn into the thylakoid lumen for reincorporation into PSII. With regard to the slightly patchy distribution of Mnx::YFP in the thylakoid membrane (Fig. 7; Supplemental Fig. S3), it could be speculated that the transporter also might localize to the biogenesis centers. More detailed studies will be necessary to identify the specific site(s) of Mnx action. We suggest that Mnx functions in parallel with PratA to provide Mn to the OEC. While, under standard conditions, the contribution of Mnx seems to be marginal in comparison with PratA in contrast to Δ*mnx* (Fig. 4C), a mutant in *pratA* has reduced photosynthetic activity (Klinkert et al., 2004), and it becomes critical under high-light conditions with increased need for PSII repair. However, the expression of *mnx* is not changed during

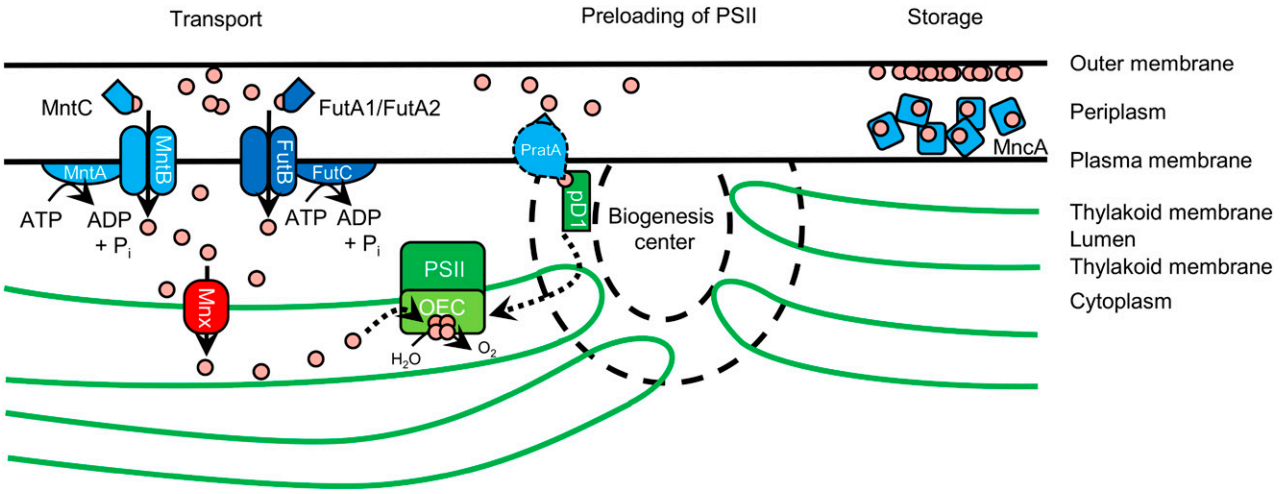

Figure 9. Hypothetical model for the function of Mnx in *Synechocystis*. Mn (Mn^{2+} ions represented as rose-colored circles; oxidation states Mn^{3+} and Mn^{4+} in the activated Mn_4O_5Ca cluster are not specifically accentuated) is stored mainly in the periplasm, with MncA as the most abundant Mn-containing protein. Mn also is suggested to bind to the outer membrane. To maintain cellular functionality, Mn is imported by the plasma membrane ABC transporter MntCAB under Mn-limiting conditions. The presence of a second, constitutively acting Mn importer has been hypothesized. Likely, the Fe ABC transporter FutABC fulfills this function. The pre-D1 (pD1) protein, which is the Mn_4O_5Ca cluster-binding core protein of PSII, is preloaded with Mn from the periplasm via PratA in biogenesis centers. The cytoplasmic surplus of Mn resulting from the turnover and degradation of Mn-containing proteins gets sequestered into the safekeeping environment thylakoid lumen via Mnx. Additionally, Mnx transports Mn from the cytoplasm into the thylakoid lumen to support Mn delivery to the OEC.

acclimation from low to high light intensities (Hihara et al., 2001). Another possible explanation for the high-light susceptibility and the retarded recovery in the Δ*mnx* mutant is that the Mn accumulation involves ROS production, as explained before, which inhibits the translation of D1 for the repair of PSII (Nishiyama et al., 2011). A more detailed analysis of PSII activity, as well as the photodamage and repair process in the mutant line, are necessary in future studies to clarify this question.

Our results indicate that both suggested biological functions of Mnx (i.e. Mn safekeeping in the thylakoid lumen and Mn provision to OEC) are critical for Mn homeostasis in *Synechocystis*. In Arabidopsis, the biological significance of the homologous thylakoid protein PAM71 is different. Since proteins homologous to PratA and biogenesis centers do not exist (Nickelsen and Rengstl, 2013), the incorporation of Mn into the OEC occurs on site in the thylakoid membrane. Mutants in *PAM71* are highly sensitive to low Mn concentrations and contain reduced amounts of Mn in isolated PSII complexes. Thus, it is suggested that PAM71 majorly serves the provision of Mn to the OEC (Schneider et al., 2016). The sequestration of surplus stromal Mn appears to be less important. This is expected because, in the highly compartmentalized plant cell, the vacuole, which is not present in cyanobacteria, serves as a reservoir for surplus metal ions, at least within physiological concentration ranges (Lanquar et al., 2010). Quite contrary to the situation in the cyanobacterial Δ*mnx* mutant, high-Mn treatment is beneficial for *pam71* mutants, since likely other, so far unknown, transporter(s) with lower affinity for Mn serve to import the Mn into the thylakoid lumen and, thereby, compensate the loss of PAM71 (Schneider et al., 2016).

Mnx Function as an Mn Transporter Is Conserved among Oxygenic Photosynthetic Organisms

The Mnx protein belongs to UPF0016, which contains only a few studied proteins. So far, only GDT1 from yeast and human TMEM165 have been investigated more closely. Both proteins are suggested to act as Ca^{2+}/H^+ antiporters in the Golgi apparatus membrane and, thus, to play important roles in Ca signaling and protein glycosylation (Demaegd et al., 2013; Colinet et al., 2016). When we treated the mutant Δ*mnx* with 12.5-fold higher concentrations of $CaCl_2$ than was used in standard BG11 medium, we did not detect any effect on the growth performance (Fig. 2B). Thus, in *Synechocystis*, Mnx is unlikely to play a major role as a Ca transporter. Interestingly, phylogenetically related proteins from green algae and land plants display similar specificity for Mn over Ca (Schneider et al., 2016). In the genome of the model plant Arabidopsis, five proteins orthologous to Mnx are encoded. Of these five proteins, PAM71 and PHOTOSYNTHESIS AFFECTED MUTANT71 HOMOLG (PAM71-HL) are targeted to the chloroplast. PAM71 resides in the thylakoid membrane and PAM71-HL in the chloroplast inner envelope (Schneider et al., 2016). The protein PAM71 was demonstrated recently to facilitate Mn uptake from the stroma into the thylakoid lumen, thus providing Mn for incorporation into the OEC of PSII (Schneider et al., 2016). Arabidopsis and

C. reinhardtii knockout mutants in this protein both could be rescued by supplementation with Mn but not Ca, emphasizing the prominent role of Mnx homologs in Mn versus Ca transport (Schneider et al., 2016). The function of PAM71-HL remains to be studied. Importantly, the duplication of plastidial Mnx homologs is conserved throughout oxygenic photosynthetic eukaryotes (Schneider et al., 2016). This indicates the importance of the role of Mnx proteins as Mn transporters in chloroplasts, the cellular compartment where oxygenic photosynthesis takes place and, thus, makes Mn management a critical task. It remains to be clarified whether the other three Mnx homologs in Arabidopsis, which are predicted to reside in membranes of the secretory pathway (Schneider et al., 2016), function in Ca or Mn transport.

CONCLUSION

In this study, we identified and characterized the Mn transport protein Mnx in the cyanobacterium *Synechocystis*. Mnx resides in the thylakoid membrane and facilitates Mn export from the cytoplasm into the thylakoid lumen, first to avoid critical cytoplasmic accumulation of Mn by sequestration in the thylakoid lumen and second to back up Mn provision to the OEC. According to our results, in cyanobacteria, the cytoplasmic Mn pool must be maintained at a constant level within a narrow range. Therefore, the released Mn needs to be exported rapidly to prevent toxic accumulation. The export function of Mnx is important under standard growth conditions and becomes crucial under high-light conditions, since Mnx likely ensures Mn supply during the repair of PSII. Members of UPF0016 are widespread among all classes of organisms. However, while, in yeast and human cells, these proteins facilitate Ca transport in the membrane of the Golgi apparatus, cyanobacterial Mnx proteins and the plant and green algal orthologous proteins that are targeted to the plastid use preferentially Mn as a transport substrate. This altered substrate specificity might be a specialization of the proteins for oxygenic photosynthetic organisms, which strongly rely on Mn.

MATERIALS AND METHODS

Synechocystis Strains and Growth Conditions

A Glc-tolerant strain of *Synechocystis* sp. PCC 6803 served as the wild type. Axenic cultures were grown continuously at 30°C, 200 rpm, and 100 μmol photons m^{-2} s^{-1} constant light in BG11 medium buffered with 20 mM HEPES-KOH to pH 7.5 (Rippka et al., 1979). Growth medium for mutant lines was supplemented with appropriate antibiotics (50 μg mL^{-1} kanamycin [Km] and 20 μg mL^{-1} spectinomycin [Sp]). For experiments, precultures were generally Mn starved for 5 d to ensure the same preconditions for all lines. To this end, the cells were washed once with EDTA solution (HEPES-KOH, pH 7.5, and 5 mM EDTA; Keren et al., 2002) and two times with Mn-free BG11 medium to remove the periplasmic storage pool of Mn. Then, the cultures were grown for 5 d in Mn-free BG11 medium and subsequently used for experiments.

Generation of *mnx* Knockout and Overexpression Lines

The Δ*mnx* knockout mutant was generated by introduction of a Km resistance cassette obtained from the plasmid pUC4K (Pharmacia) into the unique *Sma*I site of the PCR-amplified (primers ME29 and ME30; Supplemental Table S2) open reading frame *sll0615*. After transformation and selection on Km-containing BG11 plates, full segregation of several independent clones was verified by PCR analysis as described (Eisenhut et al., 2006). To generate the overexpression line Δ*mnx/OEX*, full-length *mnx* was PCR amplified using primers ME57 and ME58 (Supplemental Table S2). After digestion with *Nde*I and *Hpa*I, the *mnx* fragment was introduced into the modified version of the overexpression vector pPSBAII (Lagarde et al., 2000), carrying an Sp resistance cassette for selection (Engel et al., 2008). The obtained plasmid was used for transformation of the Δ*mnx* mutant. The complementation/overexpression line Δ*mnx/OEX* was selected on BG11 plates containing both Km and Sp.

RNA Isolation and RT-qPCR Analysis

For RNA isolation, 10 mL of culture was harvested by centrifugation for 5 min at 4°C and 3,000*g*. Extraction was performed with the Universal RNA Purification Kit (Roboklon) using the bacterial cell protocol. DNase treatment was carried out using RQ1 RNA-Free DNase (Promega), and cDNA synthesis was performed using Moloney murine leukemia virus reverse transcriptase (Promega). For the RT-qPCR analysis, Mesa Blue MasterMix for SYBR Assay (Eurogentec) was used. The primers used for RT-qPCR were FB24 and FB25 (Supplemental Table S2; efficiency, 1.94) for the amplification of *mnx*. RNase P subunit B (*rnpB*) was used as a reference gene using the primers FB26 and FB27 (Supplemental Table S2; efficiency, 1.99). RT-qPCR was performed with the StepOne Plus Real-Time system (Applied Biosystems). Mean normalized expression was calculated from three biological replicates, each measured in three technical replicates, according to Simon (2003). Samples with a cycle threshold value higher than the water control were set as not detectable.

Drop Tests

The effect of metals was tested on solid medium. Two microliters of the cultures with an OD_{750} of 0.25 and 1:10, 1:100, and 1:1,000 dilutions were spotted onto agar plates (BG11; pH 7.5; solidified with 1.5% [w/v] bacto agar), which were supplemented with different concentrations of $MnCl_2$, $CaCl_2$, FeEDTA, $CuSO_4$, $NiSO_4$, $Co(NO_3)_2$, $CdCl_2$, or $ZnSO_4$. Plates were incubated under continuous illumination of 100 μmol photons m^{-2} s^{-1} at 30°C for 4 d.

Growth, Chlorophyll, and Oxygen Evolution Analysis

After 5 d of Mn limitation, the cultures were set to an OD_{750} of 0.3 and grown in Mn-free BG11 medium for another 5 d. Then, the cultures were diluted to an OD_{750} of 0.5 and kept under limitation (0 μM $MnCl_2$) or were treated with 9 and 150 μM $MnCl_2$. Growth and chlorophyll content were determined by monitoring the OD_{750} and OD_{680}, respectively. Before and after 4 h of Mn treatment, additional samples were taken to analyze oxygen evolution as a measure of photosynthesis with a Clark-type electrode.

Effects of High-Light Treatment on Photosynthetic Activity

Cultures were set to an OD_{750} of 0.5 in BG11 medium containing the standard concentration of 9 μM $MnCl_2$. At time point 0 min, the cultures were placed under a 50-W light-emitting diode lamp at 1,000 μmol photons m^{-2} s^{-1} for 45 min. Temperature (30°C) and continuous mixing were controlled by a magnetic stirrer with heating function. After 45 min, the cultures were returned to standard growth conditions (100 μmol photons m^2 s^{-1} and 30°C) for 75 min. During the experiment, oxygen evolution as a measure of photosynthesis was analyzed every 15 min with a Clark-type electrode. The experiment was repeated three times to get biological triplicates.

Subcellular Localization of Mnx

To determine the subcellular localization of Mnx, an eYFP from pUBC-YFP-Dest (Grefen et al., 2010) was C-terminally fused to Mnx. For selection, a KmR from the vector pUC4K (Pharmacia) was added downstream of the YFP open reading frame followed by 200 bp of the 3′ region of *mnx* for homologous recombination in the *Synechocystis* genome. All fragments were PCR amplified and assembled using the Gibson Assembly Master Mix (New England Biolabs). Primers FB16 and FB17 were used to amplify *mnx*, FB18 and FB19 to amplify *yfp*, FB20 and FB21 to amplify the *KmR*, and FB22 and FB23 to amplify the 3′ region of *mnx*. Genotypes of Km-resistant transformants were verified by PCR

using primers ME57 and FB31 (Supplemental Fig. S2A), and the biological functionality of Mnx::YFP fusion proteins was tested by growth on BG11 medium supplemented with elevated $MnCl_2$ concentrations (Supplemental Fig. S2B). Before imaging, the cells were kept in darkness for 30 min to relax the proton gradient across the thylakoid membrane, because the low pH in the thylakoid lumen might affect the fluorescence of YFP. For imaging, transformed cells were mixed with wild-type cells to have a negative control in the same image. The cells were immobilized on microscopic glass slides by a thin layer of solid BG11 medium (1:1 mixture of 2-fold concentrated BG11 medium and 3% [w/v] bacto agar). A Leica TCS SP8 STED 3X microscope was used with a 100× oil objective (optical aperture 1.4) and Leica HyD hybrid detectors. YFP and chlorophyll were excited at 488 nm with a white-light laser at 70% output intensity.

ICP-MS Measurements

After precultivation under Mn limitation conditions, the cells were adjusted to an OD_{750} of 0.75 and treated with 200 μM $MnCl_2$. The higher $MnCl_2$ concentration compared with our other experiments was chosen to apply Mn stress proportional to the OD_{750} used in this experiment and thus make the effects comparable. Four-milliliter samples were pelleted via centrifugation (3,000*g* for 5 min at 4°C). The samples were washed two times with 4 mL of ice-cold EDTA solution (20 mM HEPES-KOH, pH 7.5, and 5 mM EDTA) to release the periplasmic Mn pool and measure the intracellular Mn pool only (Keren et al., 2002) and one time with 4 mL of ice-cold HEPES buffer (20 mM HEPES-KOH, pH 7.5). All steps were performed at 4°C or on ice. From here on, all steps were performed in a clean laboratory. For analysis, the samples were digested at 100°C with distilled HNO_3, evaporated to dryness, and reconstituted in double distilled water. Mn concentrations were determined using ICP-MS (PerkinElmer-Elan). For each time point, an additional sample was taken to determine the cell number per milliliter microscopically.

Radioactive Trace Experiments

After precultivation under Mn limitation conditions, the cells were adjusted to an OD_{750} of 0.3 and incubated for 3 d in BG11 medium supplemented with 0.18 μM ^{54}Mn and 0.82 μM cold ^{55}Mn. After incorporation of the radioactive Mn into the cells, the radioactive medium was washed off by one washing step with EDTA solution (20 mM HEPES-KOH, pH 7.5, and 5 mM EDTA) and two washing steps with Mn-free BG11 medium. The cultures were adjusted to an OD_{750} of 0.3 and treated with 9 μM $MnCl_2$. Samples of 500 μL were taken with a reusable syringe-type filter holder (Schleicher & Schuell) and nitrocellulose filters (Whatman). The filter residue was washed one time with EDTA solution (20 mM HEPES-KOH, pH 7.5, and 5 mM EDTA) and one time with pure water to remove the periplasmic pool of Mn. The radioactivity in the cells was monitored with a gamma counter (Kontron Analytical; GAMMAmatic I). The experiment was performed in biological triplicates, and every sample was measured in three technical replicates.

Expression of *mnx* in Yeast

The coding sequence of *mnx* was PCR amplified from *Synechocystis* genomic DNA using the primers SK102 and SK103 (Supplemental Table S2). The PCR product was subcloned into pJET1.2 (Thermo Fisher Scientific) and verified by sequencing. After restriction digestion with *Sal*I and *Spe*I, the fragment was cloned into the vector pDR196 (Rentsch et al., 1995; Loqué et al., 2007). All further experimental steps were performed as described (Schneider et al., 2016).

Supplemental Data

The following supplemental materials are available.

Supplemental Figure S1. Statistical analysis of growth rates and chlorophyll contents.

Supplemental Figure S2. Verification of the genotype and functionality of Mnx::YFP proteins.

Supplemental Figure S3. Overview of fluorescence microscopy images of wild-type and *mnx*::*yfp* cells.

Supplemental Table S1. GreenCut proteins strictly conserved in cyanobacterial genomes with predicted but so far unknown functions in chloroplast transport processes.

Supplemental Table S2. Oligonucleotides used in this study.

ACKNOWLEDGMENTS

We thank Petra Düchting (Ruhr University) and the Center of Advanced Imaging at Heinrich Heine University for excellent technical assistance.

Received December 16, 2016; accepted January 26, 2017; published January 30, 2017.

LITERATURE CITED

Anderson JM, Boardman NK, David DJ (1964) Trace metal composition of fractions obtained by digitonin fragmentation of spinach chloroplasts. Biochem Biophys Res Commun **17:** 685–689

Bartsevich VV, Pakrasi HB (1995) Molecular identification of an ABC transporter complex for manganese: analysis of a cyanobacterial mutant strain impaired in the photosynthetic oxygen evolution process. EMBO J **14:** 1845–1853

Bartsevich VV, Pakrasi HB (1996) Manganese transport in the cyanobacterium Synechocystis sp. PCC 6803. J Biol Chem **271:** 26057–26061

Clairmont KB, Hagar WG, Davis EA (1986) Manganese toxicity to chlorophyll synthesis in tobacco callus. Plant Physiol **80:** 291–293

Colinet AS, Sengottaiyan P, Deschamps A, Colsoul ML, Thines L, Demaegd D, Duchêne MC, Foulquier F, Hols P, Morsomme P (2016) Yeast Gdt1 is a Golgi-localized calcium transporter required for stress-induced calcium signaling and protein glycosylation. Sci Rep **6:** 24282

Csatorday K, Gombos Z, Szalontai B (1984) Mn and Co toxicity in chlorophyll biosynthesis. Proc Natl Acad Sci USA **81:** 476–478

Demaegd D, Foulquier F, Colinet AS, Gremillon L, Legrand D, Mariot P, Peiter E, Van Schaftingen E, Matthijs G, Morsomme P (2013) Newly characterized Golgi-localized family of proteins is involved in calcium and pH homeostasis in yeast and human cells. Proc Natl Acad Sci USA **110:** 6859–6864

Dürr G, Strayle J, Plemper R, Elbs S, Klee SK, Catty P, Wolf DH, Rudolph HK (1998) The medial-Golgi ion pump Pmr1 supplies the yeast secretory pathway with Ca^{2+} and Mn^{2+} required for glycosylation, sorting, and endoplasmic reticulum-associated protein degradation. Mol Biol Cell **9:** 1149–1162

Eisenhut M, Kahlon S, Hasse D, Ewald R, Lieman-Hurwitz J, Ogawa T, Ruth W, Bauwe H, Kaplan A, Hagemann M (2006) The plant-like C2 glycolate cycle and the bacterial-like glycerate pathway cooperate in phosphoglycolate metabolism in cyanobacteria. Plant Physiol **142:** 333–342

Engel N, Eisenhut M, Qu N, Bauwe H (2008) Arabidopsis mutants with strongly reduced levels of the T-protein subunit of glycine decarboxylase. *In* Photosynthesis: Energy from the Sun. Springer, The Netherlands. pp 819–822

Grefen C, Donald N, Hashimoto K, Kudla J, Schumacher K, Blatt MR (2010) A ubiquitin-10 promoter-based vector set for fluorescent protein tagging facilitates temporal stability and native protein distribution in transient and stable expression studies. Plant J **64:** 355–365

Hänsch R, Mendel RR (2009) Physiological functions of mineral micronutrients (Cu, Zn, Mn, Fe, Ni, Mo, B, Cl). Curr Opin Plant Biol **12:** 259–266

Hebbern CA, Laursen KH, Ladegaard AH, Schmidt SB, Pedas P, Bruhn D, Schjoerring JK, Wulfsohn D, Husted S (2009) Latent manganese deficiency increases transpiration in barley (*Hordeum vulgare*). Physiol Plant **135:** 307–316

Hihara Y, Kamei A, Kanehisa M, Kaplan A, Ikeuchi M (2001) DNA microarray analysis of cyanobacterial gene expression during acclimation to high light. Plant Cell **13:** 793–806

Houtz RL, Nable RO, Cheniae GM (1988) Evidence for effects on the in vivo activity of ribulose-bisphosphate carboxylase/oxygenase during development of Mn toxicity in tobacco. Plant Physiol **86:** 1143–1149

Karpowicz SJ, Prochnik SE, Grossman AR, Merchant SS (2011) The GreenCut2 resource, a phylogenomically derived inventory of proteins specific to the plant lineage. J Biol Chem **286:** 21427–21439

Kehres DG, Maguire ME (2003) Emerging themes in manganese transport, biochemistry and pathogenesis in bacteria. FEMS Microbiol Rev **27:** 263–290

Keren N, Kidd MJ, Penner-Hahn JE, Pakrasi HB (2002) A light-dependent mechanism for massive accumulation of manganese in the photosynthetic bacterium *Synechocystis* sp. PCC 6803. Biochemistry **41:** 15085–15092

Klinkert B, Ossenbühl F, Sikorski M, Berry S, Eichacker L, Nickelsen J (2004) PratA, a periplasmic tetratricopeptide repeat protein involved in biogenesis of photosystem II in Synechocystis sp. PCC 6803. J Biol Chem **279:** 44639–44644

Lagarde D, Beuf L, Vermaas W (2000) Increased production of zeaxanthin and other pigments by application of genetic engineering techniques to *Synechocystis* sp. strain PCC 6803. Appl Environ Microbiol **66:** 64–72

Lanquar V, Lelièvre F, Bolte S, Hamès C, Alcon C, Neumann D, Vansuyt G, Curie C, Schröder A, Krämer U, et al (2005) Mobilization of vacuolar iron by AtNRAMP3 and AtNRAMP4 is essential for seed germination on low iron. EMBO J **24:** 4041–4051

Lanquar V, Ramos MS, Lelièvre F, Barbier-Brygoo H, Krieger-Liszkay A, Krämer U, Thomine S (2010) Export of vacuolar manganese by AtNRAMP3 and AtNRAMP4 is required for optimal photosynthesis and growth under manganese deficiency. Plant Physiol **152:** 1986–1999

Lapinskas PJ, Cunningham KW, Liu XF, Fink GR, Culotta VC (1995) Mutations in *PMR1* suppress oxidative damage in yeast cells lacking superoxide dismutase. Mol Cell Biol **15:** 1382–1388

Liberton M, Saha R, Jacobs JM, Nguyen AY, Gritsenko MA, Smith RD, Koppenaal DW, Pakrasi HB (2016) Global proteomic analysis reveals an exclusive role of thylakoid membranes in bioenergetics of a model cyanobacterium. Mol Cell Proteomics **15:** 2021–2032

Loqué D, Lalonde S, Looger LL, von Wirén N, Frommer WB (2007) A cytosolic trans-activation domain essential for ammonium uptake. Nature **446:** 195–198

Lynch JP, St. Clair SB (2004) Mineral stress: the missing link in understanding how global climate change will affect plants in real world soils. Crop Res **90:** 101–115

Maeda T, Sugiura R, Kita A, Saito M, Deng L, He Y, Yabin L, Fujita Y, Takegawa K, Shuntoh H, et al (2004) Pmr1, a P-type ATPase, and Pdt1, an Nramp homologue, cooperatively regulate cell morphogenesis in fission yeast: the importance of Mn^{2+} homeostasis. Genes Cells **9:** 71–82

Millaleo R, Reyes-Díaz M, Alberdi M, Ivanov AG, Krol M, Hüner NP (2013) Excess manganese differentially inhibits photosystem I versus II in *Arabidopsis thaliana*. J Exp Bot **64:** 343–354

Nable RO, Houtz RL, Cheniae GM (1988) Early inhibition of photosynthesis during development of Mn toxicity in tobacco. Plant Physiol **86:** 1136–1142

Nelson N, Junge W (2015) Structure and energy transfer in photosystems of oxygenic photosynthesis. Annu Rev Biochem **84:** 659–683

Nickelsen J, Rengstl B (2013) Photosystem II assembly: from cyanobacteria to plants. Annu Rev Plant Biol **64:** 609–635

Nishiyama Y, Allakhverdiev SI, Murata N (2011) Protein synthesis is the primary target of reactive oxygen species in the photoinhibition of photosystem II. Physiol Plant **142:** 35–46

Ogawa T, Bao DH, Katoh H, Shibata M, Pakrasi HB, Bhattacharyya-Pakrasi M (2002) A two-component signal transduction pathway regulates manganese homeostasis in *Synechocystis* 6803, a photosynthetic organism. J Biol Chem **277:** 28981–28986

Rentsch D, Laloi M, Rouhara I, Schmelzer E, Delrot S, Frommer WB (1995) NTR1 encodes a high affinity oligopeptide transporter in *Arabidopsis*. FEBS Lett **370:** 264–268

Rippka R, Deruelles J, Waterbury JB, Herdman M, Stanier RY (1979) Generic assignments, strain histories and properties of pure cultures of cyanobacteria. J Gen Microbiol **111:** 1–61

Rosch JW, Gao G, Ridout G, Wang YD, Tuomanen EI (2009) Role of the manganese efflux system *mntE* for signalling and pathogenesis in *Streptococcus pneumoniae*. Mol Microbiol **72:** 12–25

Salomon E, Keren N (2011) Manganese limitation induces changes in the activity and in the organization of photosynthetic complexes in the cyanobacterium *Synechocystis* sp. strain PCC 6803. Plant Physiol **155:** 571–579

Salomon E, Keren N (2015) Acclimation to environmentally relevant Mn concentrations rescues a cyanobacterium from the detrimental effects of iron limitation. Environ Microbiol **17:** 2090–2098

Schneider A, Steinberger I, Herdean A, Gandini C, Eisenhut M, Kurz S, Morper A, Hoecker N, Rühle T, Labs M, et al (2016) The evolutionarily conserved protein PHOTOSYNTHESIS AFFECTED MUTANT71 is required for efficient manganese uptake at the thylakoid membrane in *Arabidopsis*. Plant Cell **28:** 892–910

Sharon S, Salomon E, Kranzler C, Lis H, Lehmann R, Georg J, Zer H, Hess WR, Keren N (2014) The hierarchy of transition metal homeostasis: iron controls manganese accumulation in a unicellular cyanobacterium. Biochim Biophys Acta **1837:** 1990–1997

Simon P (2003) Q-Gene: processing quantitative real-time RT-PCR data. Bioinformatics **19:** 1439–1440

Socha AL, Guerinot ML (2014) Mn-euvering manganese: the role of transporter gene family members in manganese uptake and mobilization in plants. Front Plant Sci **5:** 106

Stengel A, Gügel IL, Hilger D, Rengstl B, Jung H, Nickelsen J (2012) Initial steps of photosystem II de novo assembly and preloading with manganese take place in biogenesis centers in *Synechocystis*. Plant Cell **24:** 660–675

Tobergte DR, Curtis S (2012) Marschner's Mineral Nutrition of Higher Plants. Academic Press, United Kingdom

Tottey S, Waldron KJ, Firbank SJ, Reale B, Bessant C, Sato K, Cheek TR, Gray J, Banfield MJ, Dennison C, et al (2008) Protein-folding location can regulate manganese-binding versus copper- or zinc-binding. Nature **455:** 1138–1142

Tsunekawa K, Shijuku T, Hayashimoto M, Kojima Y, Onai K, Morishita M, Ishiura M, Kuroda T, Nakamura T, Kobayashi H, et al (2009) Identification and characterization of the Na^+/H^+ antiporter Nhas3 from the thylakoid membrane of *Synechocystis* sp. PCC 6803. J Biol Chem **284:** 16513–16521

Yamaguchi K, Suzuki I, Yamamoto H, Lyukevich A, Bodrova I, Los DA, Piven I, Zinchenko V, Kanehisa M, Murata N (2002) A two-component Mn^{2+}-sensing system negatively regulates expression of the *mntCAB* operon in *Synechocystis*. Plant Cell **14:** 2901–2913

Zorina A, Sinetova MA, Kupriyanova EV, Mironov KS, Molkova I, Nazarenko LV, Zinchenko VV, Los DA (2016) *Synechocystis* mutants defective in manganese uptake regulatory system, ManSR, are hypersensitive to strong light. Photosynth Res **130:** 11–17